SPERT I Reactor Safety Studies

By W. E. Nyer and S. G. Forbes*

The principal safety problems associated with the operation of nuclear reactors are concerned with the ways in which a reactor itself brings about widespread movement of fission products. Reactor runaway is one of the most important of these because it is possible to achieve such rapid increases of power that the energy in the system accumulates much faster than it can be removed and this accumulated energy can reach disastrous proportions before external controls can be effective. Another characteristic related to reactor safety, that of possible instability, is not unique to reactors. This is most frequently regarded as a problem in plant operation, but it is also a safety problem because reactor instability may be a means of initiating a runaway.

These problems involve aspects of the kinetic behavior of reactors, hence the understanding of kinetic behavior can be expected to contribute greatly to reactor safety. The results of experimental studies of reactor kinetic behavior under runaway conditions are reported here for the unpressurized SPERT I reactor.

The initiation of a runaway may occur in numerous ways, but each of these can be characterized as a reactivity disturbance under a particular set of initial conditions of the reactor system. The disturbance must be further specified by its magnitude and speed of occurrence, which in practice brings into consideration the various means of reactivity introduction and their probabilities of occurrence. Subsequent to the reactivity disturbance, events are determined by the response characteristics of the reactor system, which are a combination of the largely non-nuclear characteristics of appendages like the control system, and inherent characteristics which are strongly nuclear. In the most extreme accident cases the sequence of events will be too rapid for effective control by external means. Then, the course of the response will be fully determined by the inherent characteristics and the safety of the system depends on the self-limiting characteristics of the reactor response. The culminating events may include a breach of the primary container and the dispersion of fission products. Reduction of the probability of occurrence of an accident and improvements in the inherent response characteristics are accident prevention measures while containment and site isolation are essentially means of coping with the consequences of an accident.

The experiments reported here were concerned mainly with the study of reactor response characteristics under runaway conditions and the immediate consequences of the accident, such as fuel plate melting or mechanical damage. Other important factors which must be taken into account in assessing the safety of reactors, such as the effectiveness of containment measures, and the probability of occurrence of the incident, are not discussed herein.

The great variety of conceivable forms of the reactivity disturbance in the initiation phase can be effectively represented by the two forms used in the experiments. The severest condition is that for which a given reactivity is inserted effectively instantaneously—that is, as a step-function. This is representative of the initial conditions of a severe accident. Tests of this sort will be referred to as step-transients. In the other form, which is typical of many postulated accidents, reactivity is added to the reactor system at a constant rate. These will be referred to as ramp-transient tests and the rate of addition of reactivity will be referred to as ramp rate or assembly rate. The assembly rates that can be produced by external operations or by internal behavior can in fact approach step-functions.

SPERT I FACILITIES AND CORES

Since the SPERT facilities, equipment and experimental technique have been described in detail elsewhere[1], only a brief summary of these will be included here. The SPERT I reactor core is contained in an open tank 4 ft in diameter and 10 ft high. This tank is normally filled to a point about 2 ft above the top of the core with light water which serves as moderator and reflector. There are five blade-type poison rods. The outer four serve as control rods. The central transient rod, which in its normal rest position has the cadmium portion below the reactor core, is raised to bring poison into the core. Transients are initiated either by releasing the suspended transient rod and driving it downward out of the reactor for step tests or by steady withdrawal of the bank of four control rods for ramp tests.

Two types of fuel assemblies were used in the various cores. Each type was a box-form with nominal dimensions of 3 in. by 3 in. by 24 in. long. Type A

* Phillips Petroleum Company, Atomic Energy Division, Idaho Falls, Idaho.

assemblies consisted of 17 rows of fuel plates. Each row consists of three plates nominally 1 in. wide brazed into aluminium side plates. This is referred to as a 17-plate assembly. Type B assemblies consisted of four permanently brazed-in fuel plates nominally 3 in. wide, and 20 removable plates to permit variations in the number of plates per assembly, and thus in the thickness of the gap between plates. Each plate consists of enriched uranium–aluminum alloy 0.020 in. thick clad with 0.020 in. of aluminum.

The different assemblies were used to form cores which ranged from under-moderated to slightly over-moderated. The core configurations are shown in Fig. 1; the heavy outline encloses the critical loading. Cores are designated by the type of fuel assembly, the number of 3 in. wide fuel plates per assembly, and the number of assemblies per core. Fuel assembly data and experimentally determined core characteristics are given in Table 1. As shown there, changing cores produced changes in characteristics of importance in kinetic behavior. The prompt neutron life-time ranged from about 75 μsec for the 12-plate core to 50 μsec for the 24-plate core. Correspondingly, the void coefficient ranged from -0.6×10^{-4} % $\Delta k/cm^3$ of void to -5×10^{-4} % $\Delta k/cm^3$ of void. The 12-plate core exhibited local positive reactivity effects in the neighbourhood of the central cross. The variations in the thickness of the water channels between fuel plates ranged from about 60 mils to about 190 mils.

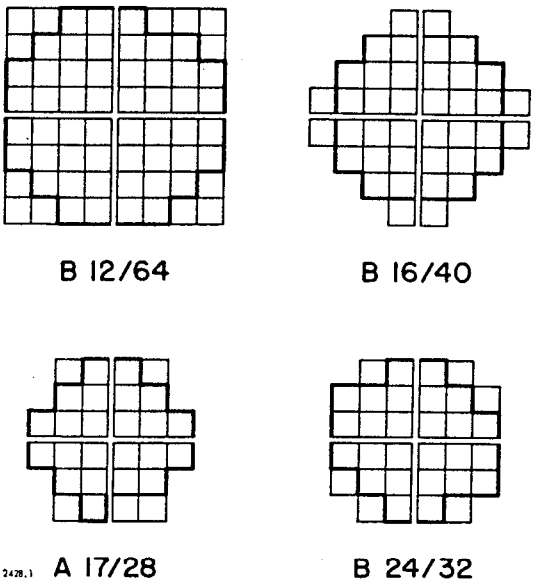

Figure 1. SPERT I core configurations: each square represents a fuel assembly. The heavy outline shows the critical configuration

STEP TRANSIENTS

Previously reported studies[2] described in detail the characteristics and variations of reactor transient behavior over a wide range of initial asymptotic periods for the A-17/28 core. In the present paper the effects on burst behavior produced by changes in some core characteristics and by changes in the initial reactor temperature are presented for comparable ranges of initial periods.

The step-transient tests were performed according to the following procedure. The reactor temperature and water head were adjusted to the desired values. Then, with the reactor slightly subcritical at a low power (several watts), reactivity was introduced effectively instantaneously by the rapid ejection of the transient rod.

Typically, the reactor power history during a transient or burst is the following: A short time after the ejection of the transient rod, the power rise becomes exponential with a period τ, determined by the reactivity addition. The exponential rise continues until the energy accumulated in the shutdown mechanisms is sufficient to cause an appreciable reduction in the reactivity of the system. As the reactivity continues to decrease, the power passes through a maximum and thereafter approaches a quasi-equilibrium value either monotonically or in an oscillatory fashion. The tests are usually terminated by a programmed scram shortly after the initial burst. In all cases the initial burst is controlled by the self-limiting

Table 1. Characteristics of SPERT I Cores

Fuel Assemblies	*B-25*	*A-17*	*B-16*	*B-12*
No. of fuel plates	24	51	16	12
Gap between plates, mils	65	117	190/65[a]	190
Heat transfer area meters²/assembly	1.8	1.5	1.2	0.9
Metal/water ratio 3 in. × 3 in. × 24 in. cell	1.14	0.79	0.63	0.46
Grams U^{235}/plate	7.0	3.3	7.0	7.0
Core (Type, No. of plates per assembly and No. assemblies in full core)	B-24/32	A-17/28	B-16/40	B-12/64
Critical mass	4.3 kg	3.9 kg	3.6 kg	4.0 kg
$\%\Delta k$ loss from temperature 20°C to 95°C	1.21	1.10	1.17	1.01
Average void coefficient $\%\Delta k/cm^3$	-5.1×10^{-4}	-3.5×10^{-4}	-2.0×10^{-4}	-0.65×10^{-4}
Central void coefficient $\%\Delta k/cm^3$	-12×10^{-4}	-7×10^{-4}	-3.3×10^{-4}	$+0.55\times10^{-4}$
Max. negative void coefficient $\%\Delta k/cm^3$	-12×10^{-4}	-7×10^{-4}	-4.1×10^{-4}	-0.9×10^{-4}
Max. positive void coefficient $\%\Delta k/cm^3$	none	none	none	4.2×10^{-4}
Prompt neutron lifetime[b] μsec	49	48	72	75
Average heat coefficient $\%\Delta k$/Mw-sec	-4.7×10^{-2}	-4.2×10^{-2}	-3.1×10^{-2}	-1.8×10^{-2}

[a] Alternate wide and narrow channels.
[b] Best fit to experimental data using $\beta=0.007$

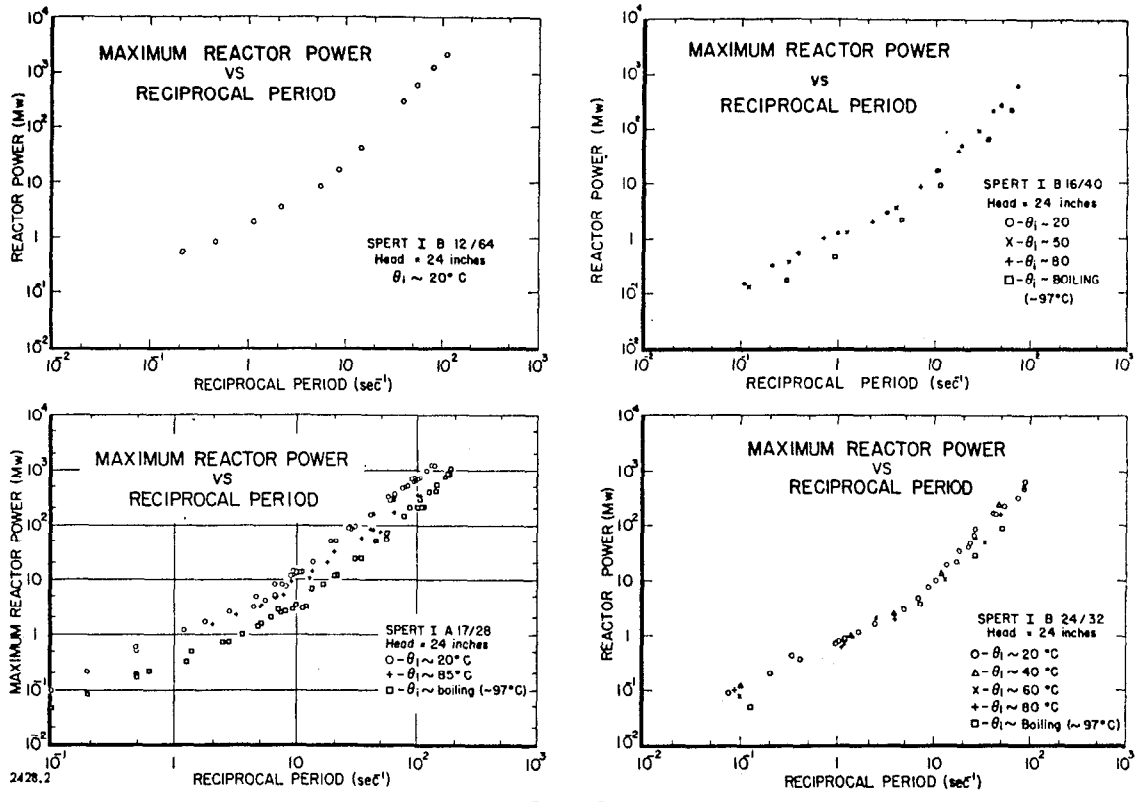

Figure 2

characteristics of the reactor without application of external controls.

Neutron flux, fuel plate temperatures, and transient pressures are the primary measurements made during the power excursions.[3] The neutron flux measurements are made at a point outside the reactor tank by boron-lined ion chambers which have been calibrated in terms of the total reactor power by calorimetric techniques. Temperatures are measured at selected points in the core by thermocouples attached to the fuel plate surfaces. Pressure transducers mounted in the end boxes at the bottom of fuel assemblies provide transient pressure information. All signals are recorded one-half mile away at the Control Center on multi-channel oscillographs. The transient response of the combined electronic-galvanometer system is such that a 1-msec period can be followed with negligible distortion.

A number of characteristics of the series are conveniently presented as functions of α, the reciprocal of the initial period. Figures 2 through 6 display for each of the four cores, the peak power, energy release to time of peak power, temperature rise at time of peak power, maximum temperature and maximum pressure respectively, versus α, with the initial reactor bulk temperature, θ_1, as a parameter. Generally, data points are plotted to give an indication of the spread in the experimental results, which was greater than the experimental error in the individual measurements. In a few cases line-average plots are used for clarity. The pattern of behavior for these cores does not differ markedly from that reported earlier for the 20°C series with the A-17/28 core.

The peak-power plots in Fig. 2 all exhibit a dependence on α which in the long period region is almost linear and which in the short period region is nearly quadratic. The existence of a break-point separating the two regions is clear. Its location is not sharply defined but in all cases is in the neighborhood of five reciprocal seconds. An increase in the initial temperature to boiling resulted in an almost constant downward displacement of the curve for the A-17/28 core. Tests initiated from 85°C show a gradual transition for the 20°C characteristic to the boiling characteristic as α increases.

The effects of initial temperature on the energy release are more pronounced than on the peak power. This is indicative of a temperature effect on burst shape. The variation with temperature is greatest at small α with an indication that at large α the characteristics are merging. Again, the test results at intermediate temperature show a transition from the 20°C line at low α to the boiling curve at high α. The characteristic form of the energy release curve with the minimum in the neighborhood of α equal to five is clear for the 20°C curve and clearly suggested in all others.

The behavior of the fuel plate temperature rise at the time of peak power and the maximum fuel plate temperature, as shown in Figs. 4 and 5, respectively, is consistent with the foregoing. Again at α about 5 the slopes of the plots show a sudden increase. As

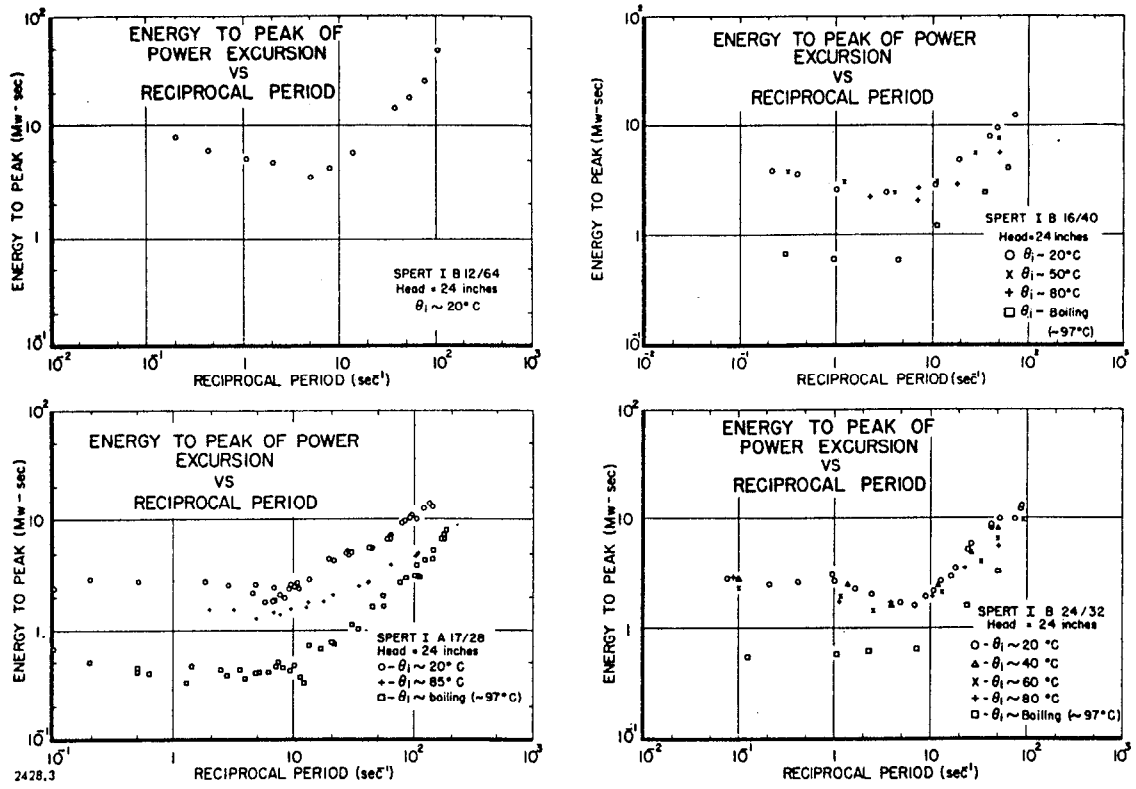

Figure 3

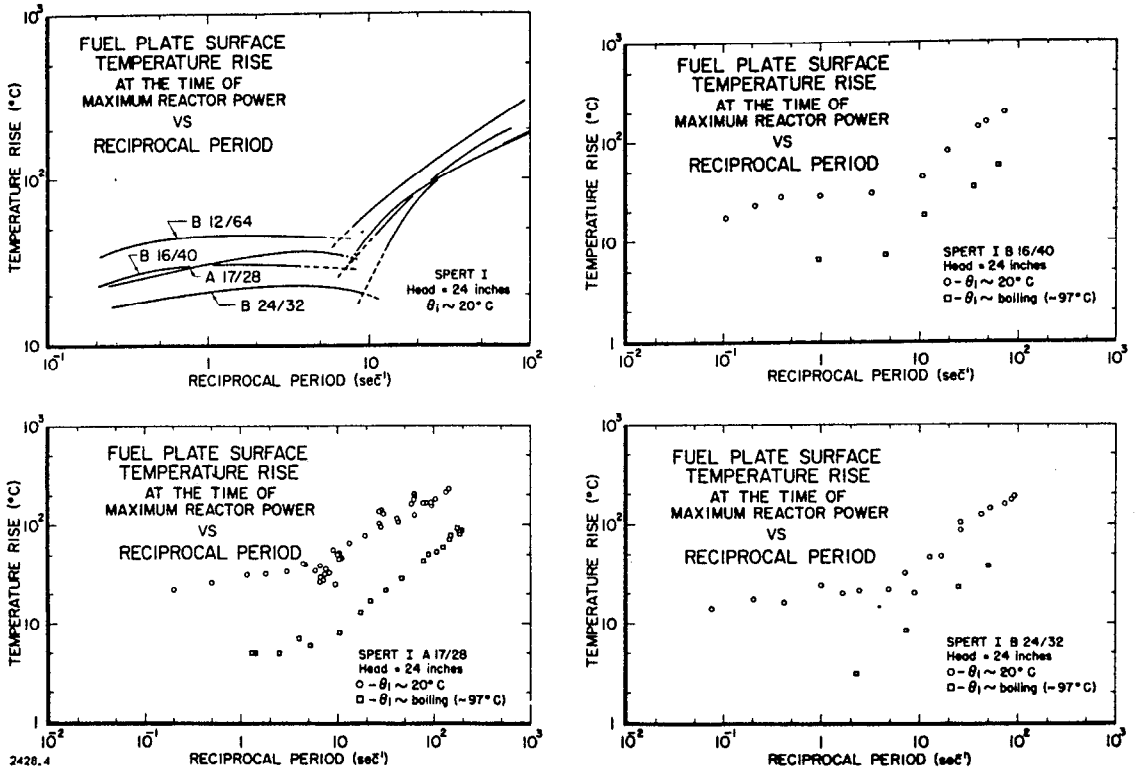

Figure 4

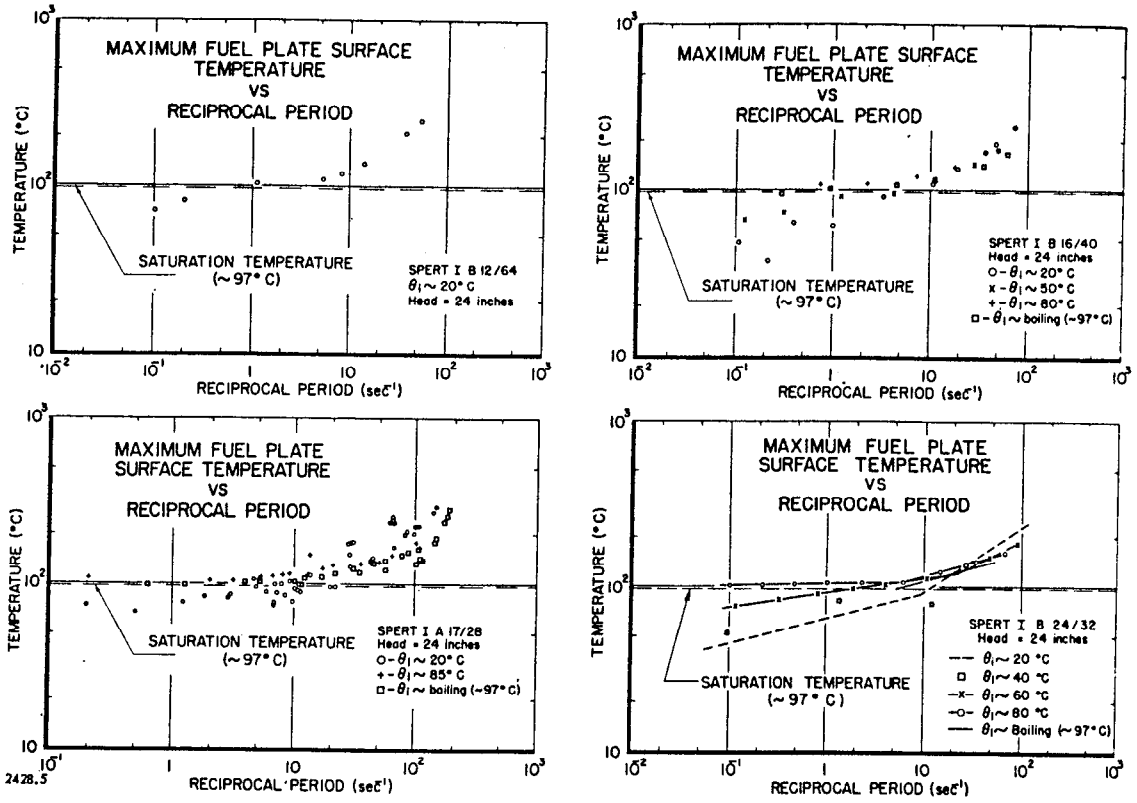

Figure 5

described in detail in Ref. 2, the maximum temperature occurs significantly after the power maximum except at very short periods and does not have much significance at long periods other than as a practical safety guide in the conduct of the experiments.

Pressure measurements are made at selected points and can be expected to exhibit greater variation than the power measurements which integrate over the entire core. The scatter of the individual pressure points in Fig. 6 is an indication of the qualitative nature of these results. The pressure peaks generally occur after power peaks but the lag becomes negligible at short periods where the pressure rise is most noticeable. The peak pressure varies approximately as α^2 over the range of measurements, but there is an indication that the function rises more steeply at higher α. At a given α, the peak pressure decreases as the plate spacing increases. The onset of measurable pressures is not accompanied by any apparent change in the characteristics of the burst up to the time of peak. This is consistent with the time-behavior of the pressure during a burst which shows that in most excursions the power has nearly reached the peak value before a sizable pressure rise occurs.

Figure 6 also shows the peak power curves for the four cores at the initial temperature of 20°C. The decrease in the reactivity coefficient (Table 1) is seen to be accompanied by an upward displacement of the peak power curve.

The last set of curves in Fig. 6 shows for comparison the energy release up to the time of peak power, $E(t_m)$, and the reactivity compensated at the time of peak power, $k_c(t_m)$, for the 20°C tests with the 12- and 17-plate cores. The behavior of both functions is quite similar. The compensated reactivity, $k_c(t)$, was computed from the experimentally observed power histories,[4] using the neutron kinetic equations. The near-constancy of the displacement of the energy curves from their corresponding reactivity curves indicates that for a particular core the effective average dynamic reactivity coefficient at the time of peak power is nearly constant for all α. The coincidence of the reactivity curves at small α implies a constancy of burst-shape for both cores. At larger α these curves separate but the effect is due to the manner of plotting which introduces a scale factor proportional to the prompt neutron lifetime. The initial reactivity curve, $k(0)$, is an in-hour plot with $\beta=0.007$ and $\ell=50$ μsec. This represents an upper limit to the reactivity which must be compensated by the reactor system to stop an excursion in the absence of effects which are autocatalytic or which permit the escape of shutdown energy from the system.

A number of the features of the experimental data can be accounted for by rather simple theoretical considerations. The region of principal interest from a safety standpoint is that above prompt critical where the pressure and temperature approach damaging levels. For this case delayed neutrons may be ignored and the neutron kinetic equation written:

$$\frac{\ddot{\phi}(t)}{\phi(t)} = \alpha(t) \qquad (1)$$

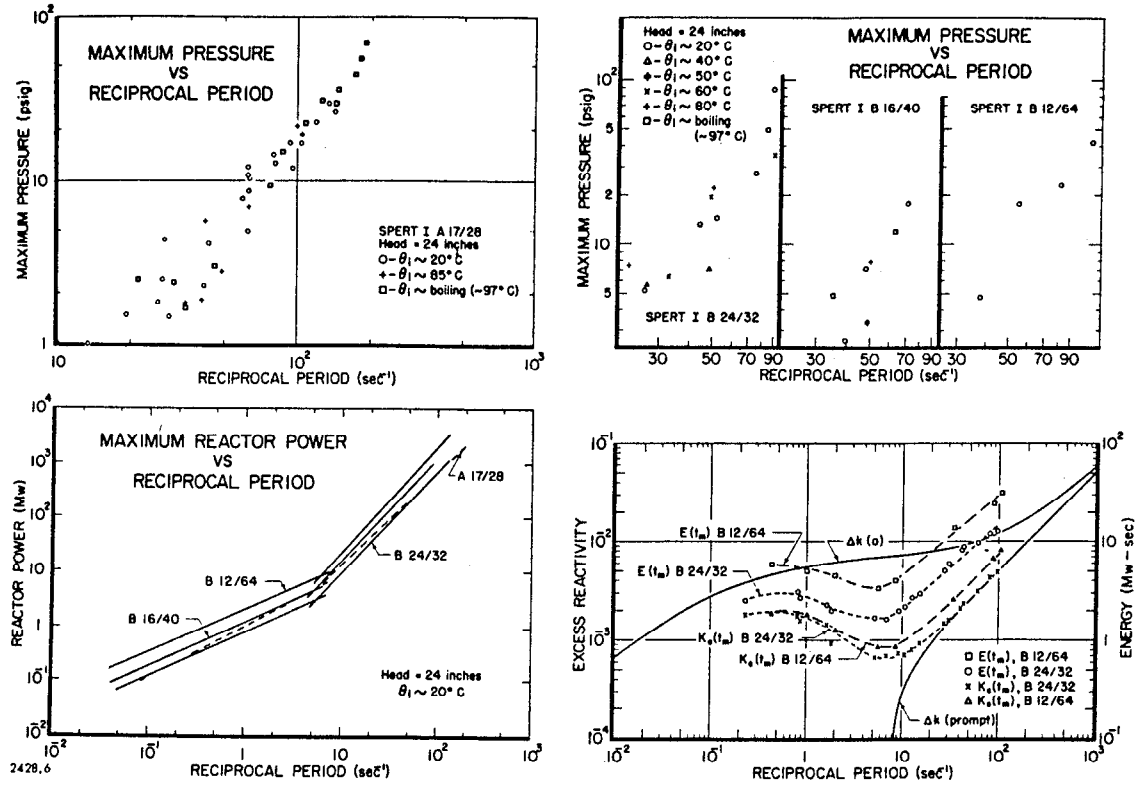

Figure 6

where $\phi(t)$ is the energy release at time t and the dots indicate time derivatives. $\alpha(t)$ is thereby defined as the instantaneous slope of a logarithmic plot of the power. For an exponential power rise α, the reciprocal of the period τ, is equal to the prompt reactivity Δk_p, divided by the prompt neutron lifetime ℓ. If $\alpha(t)$ is assumed to be equal to $\Delta k_p(t)$ divided by ℓ for all t, it is thereby coupled to the power history of the burst because the energy release results in a reactivity change.

The problem of selecting the proper form of the equation coupling the reactivity change to the power history may be sidestepped by assuming an analytical form (e.g., a simple exponential) for the power burst up to the peak. The shutdown effect is computed on the basis of an assumed shutdown mechanism and the burst is terminated when the reactivity is reduced to zero. Values of peak power, temperature, etc., can then be computed. The experimental data can be matched reasonably well by a number of different assumed mechanisms but this does not provide a basis for selection from among these mechanisms. The neglect of coupling effects does not provide details of behavior during the burst, thus eliminating valuable points of comparison with the experimental data.

Alternatively, Eq. (1) may be combined with a coupling equation to provide descriptions of the burst behavior.

Analytical results have been obtained[5] by the use of a coupling equation which is a simple function of the energy released by the reactor. The resulting equation for step transients may be written:

$$\frac{\ddot{\phi}(t)}{\dot{\phi}(t)} = \alpha_0 - b\,[\phi(t-T)]^n \qquad (2)$$

where α_0 is proportional to the injected reactivity, b is the reactivity coefficient in units of energy^{-n} sec^{-1} $\phi(t-T)$ indicates that the shutdown effect at time t lags the energy release by a time T; and n is an exponent expressing a simple power law relation between the shutdown effect and the energy release. Analytical forms for the power and reactivity compensation as functions of time have been obtained for all values of n with the delay time T both zero and long compared to the reactor period. The best agreement with the experimental data is obtained from the analytical form for the long delay time T, with the exponent n, between 1.5 and 2. The agreement is sufficiently good that the analytical equations can be used as a point of comparison in the selection of the physical mechanisms responsible for shutdown.

Both the zero- and long-delay models predict that peak power and energy release at peak power will be proportional to $b^{1/n}$, indicating a relatively weak dependence on the shutdown coefficients. The long-delay model permits the introduction of an α_0 dependence in the time delay term T. In order to produce agreement with the experimentally observed peak power versus α and energy release versus α data, the required time delay function $T(\alpha_0)$ must be approximately constant in terms of reactor periods.

In summary, agreement between theory and experiment in the prompt region can be obtained from a simple delayed energy shutdown model.

The extension of these results to the long period region requires the inclusion of delayed neutrons in the kinetic equation. A calculated peak-power versus α curve in good agreement with the experimental shape was obtained by Griffing[6] for the prompt and delayed neutron regions using a linear relation between reactivity loss and energy release. This did not produce agreement in detail with experiment but the observed shape of the peak power and $E(t_m)$ curves can be reproduced. Thus, a change in shutdown mechanisms at the break point need not be invoked to explain the changes in slope although this possibility is not excluded. On general grounds a lower limit to the $k_c(t_m)$ curve can be constructed[5] which exhibits a dip in the region of prompt critical. Corben[7] has shown that a similar form can be obtained analytically for a whole class of coupling equations. Thus the main features of the $k_c(t_m)$ curves are properties of the kinetic equations rather than of the shutdown mechanisms.

Some implications of theory and experiment for reactor safety should be noted. The theoretical results are independent of the reactor system since they basically depend only on the constancy of the burst shape. Thus, the runaway behavior of reactors with similar properties could, with reasonable accuracy, be predicted from a simple measurement of the effective dynamic reactivity coefficient.

The identification of the primary shutdown mechanism is not materially aided by these considerations, which are theories of the form of the energy transfer, because of the difficulty of excluding any particular mechanism. For the same reason, the values of the effective dynamic reactivity coefficients computed from the $k_c(t_m)$ and $E(t_m)$ curves in Fig. 6 do not assist in settling this point.

In addition, the small values of reactivity compensation required below prompt critical suggest that control of reactivity perturbations up to prompt critical can be achieved by emphasizing the speed of controls rather than the magnitude of reactivity control.

RAMP TRANSIENTS

The results from a small number of ramp-rate tests with the A-17/28 core have been reported.[8] This portion of the paper will present additional results obtained with the same core.

The burst behavior in the type of accident initiated by a ramp-rate insertion of reactivity can be expected to differ from that of a burst induced by a step-function input of reactivity and to depend on different parameters. The initial power, which is unimportant in the step case provided only that it is very low, becomes an important parameter in ramp tests. In addition, the slope of the ramp function can be expected to exert strong influence on the course of an accident. Further, the long time-scale for moderately slow ramp tests relative to step tests should produce smaller bursts. However, if extremely fast assembly rates are permitted for ramp tests, the severity of ramp accidents can be as great as for step accidents.

Changes in the previously described experimental technique were made to adapt it to the investigation of

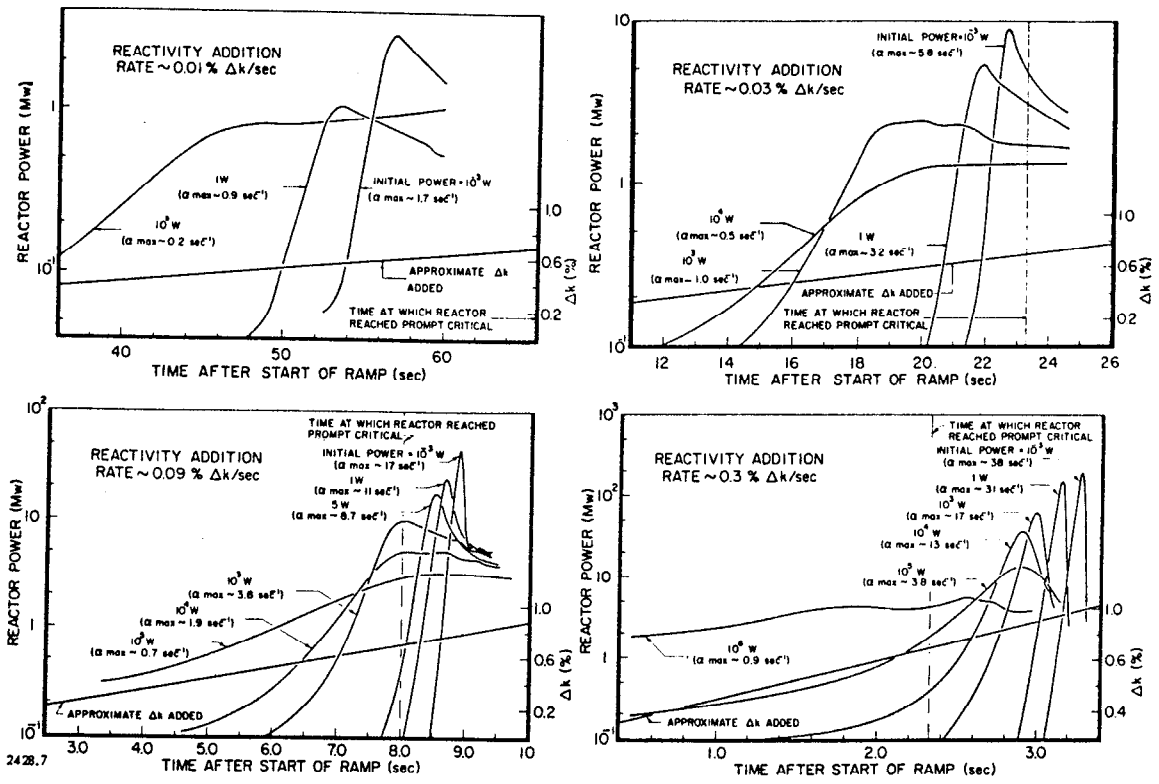

Figure 7

this type of behavior but equipment limitations made it impossible to control the initial conditions to the extent desired. The tests were started with the reactor somewhat sub-critical at a reasonably steady power. The transient rod was then ejected to make the system critical and, at the same time, withdrawal of the control rods was begun.

Typical logarithmic plots of the reactor power show at first a rising power with a slope that gradually increases to a maximum, then decreases to zero at the time of the power maximum. In most cases, the power behavior after the initial burst is more characteristic of the total reactivity in the system than of the manner of introduction and is thus primarily a stability problem. This discussion, as in the case of step transients, is concerned primarily with the initial burst.

Figure 7 shows the power behavior produced by steady reactivity insertion rates of 0.01% Δk/sec, 0.03% Δk/sec, 0.09% Δk/sec, and 0.3% Δk/sec, respectively, for different values of the initial power. The effect of decreasing starting power is to increase the peak power and to delay the time at which it occurs. Increasing the ramp rate raises the peak and decreases the time required to reach it.

It may be seen from Fig. 8 that the ramp rate is a more important parameter than initial power. In addition, Fig. 8 shows a plot of the maximum power in a ramp-induced burst as a function of the minimum period. The solid line represents the peak-power versus α curve for step insertion tests with the same core. The underlined data points were reported earlier.[8]

Analytical results can be obtained for the prompt neutron approximation when the reactivity insertion function is a ramp-rate.[5] The appropriate equations are the following:

$$\frac{\ddot{\phi}}{\phi} = \alpha(t) = at - b\phi(t) \qquad (3)$$

where the newly introduced symbol a is the rate of addition of reactivity, k, divided by ℓ. The equation predicts that α reaches a maximum value, α_m when the power $\phi(t)$ has risen to a value:

$$\phi_m = \frac{a}{b}. \qquad (4)$$

At this time $\alpha(t_m) \equiv \alpha_m$ and is given by:

$$\alpha_m \simeq \sqrt{2a\left(\ln\frac{a}{b\phi(0)} - 1\right)} \qquad (5)$$

provided that $\phi(0)$ is less than $0.1\phi_m$.

Comparison of (4) and (5) with the experimental results for tests in which the maximum period was substantially less than the prompt critical period show qualitative agreement with the predictions that ϕ_m is independent of $\phi(0)$ and that α_m depends more strongly on a than on b. Estimates of value of b from

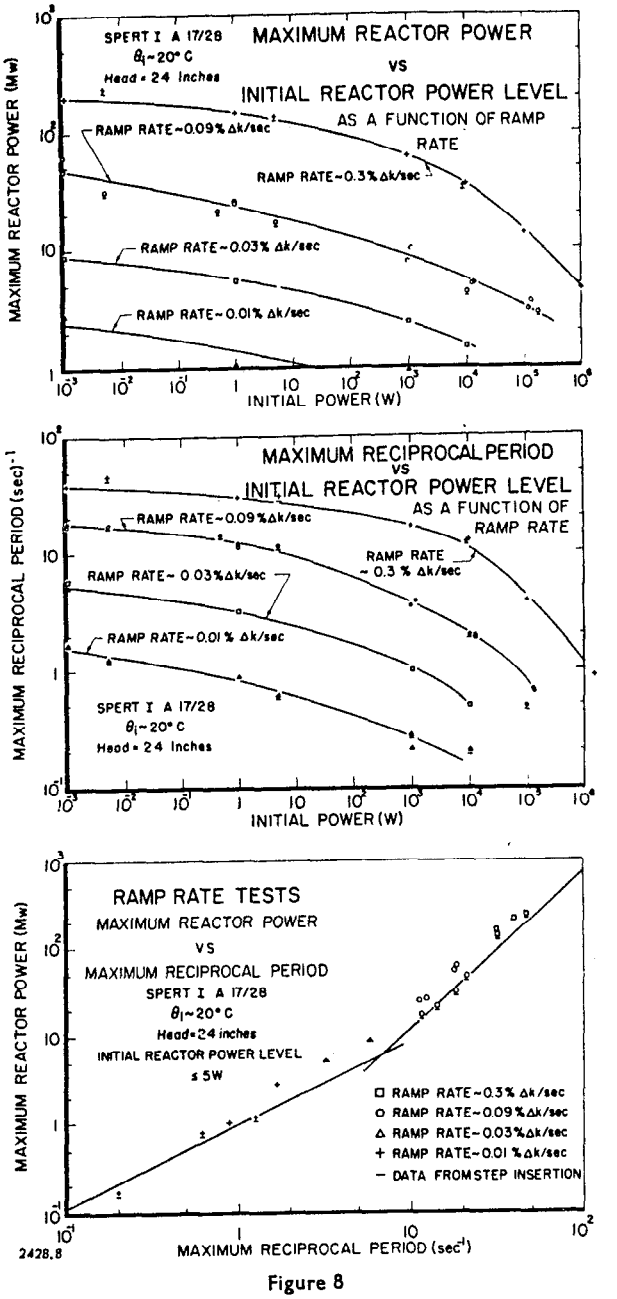

Figure 8

(4) using the experimental values of ϕ_m are within a factor of two of the effective dynamic coefficients for step-transient tests.

The work of Forbes on step transients[5] is in accord with this observation.

The theory and experimental results on ramps can serve as a practical guide in establishing safety requirements for source strength and permissible control-rod withdrawal rates.

Indeed, the safety aspect of the ramp- and step-transient experiments can be emphasized by noting that it is possible to construct an always-safe reactor,[9] within suitable restrictions. A relaxation of the restrictions by increased knowledge is an objective of this work.

REFERENCES

1. T. R. Wilson, *An Engineering Description of the Spert I Reactor*, IDO-16318 (14 June 1957).
2. F. Schroeder, S. G. Forbes, W. E. Nyer, F. L. Bentzen and G. O. Bright, *Experimental Study of Transient Behavior in a Subcooled, Water-Moderated Reactor*, Nuclear Sci. and Eng., 2, 96–115 (1957).
3. F. L. Bentzen, *Spert I Instrumentation*, IDO-16316 (15 March 1957).
4. R. W. Miller, *Calculations of Reactivity Behavior During Spert I Transients*, IDO-16317 (1 June 1957).
5. *Spert Quarterly Progress Report—January, February, March, 1958*, IDO-16452.
6. G. W. Griffing and L. I. Deverall, *Kinetic Studies on Spert I Reactor – Initial Behavior by Energy Model*, IDO-16397 (18 April 1958).
7. H. C. Corben, *Power Bursts in Nuclear Reactors*, presented at the 1958 Annual Meeting of the American Nuclear Society (2–5 June, Los Angeles, California); H. C. Corben and W. Horning, *Theory of Power Transients in the Spert I Reactor*, IDO-16434 (10 January 1958).
8. W. E. Nyer, S. G. Forbes, F. L. Bentzen, G. O. Bright, F. Schroeder and T. R. Wilson, *Experimental Investigations of Reactor Transients*, IDO-16285 (June 1956).
9. W. E. Nyer and S. G. Forbes, *The Role of Reactor Kinetic Behavior in Reactor Safety*, presented at the Reactor Safety Conference in New York City, New York (31 October 1957).

Mr. Nyer presented Paper P/2428, above, at the Conference, and added the following remarks: The simple linear mathematical model, mentioned in the paper, predicts that the energy and power at the time of the power peak should be proportional to the reactivity coefficient. The experimental data exhibit a more nearly square root dependence. The theory can be modified to predict this dependence by assuming that the reactivity loss depends on the nth power of the energy released and by introducing a time delay between energy release and reactivity change.

A more detailed comparison of theory with experiment is possible by consideration of the time behavior of power and compensated reactivity during a burst. Figure 9 compares power burst shapes for different values of the exponent, n, for a zero time-delay model with a burst having an initial period of 9.5 milliseconds. The ordinate shows the logarithm of relative power and the abscissa shows time, x, in units of reactor periods. The solid lines are the calculated curves for several values of n and the points represent experimental data. For n equal to two, the fit up to the peak of burst is good, whereas the fit after the peak is poor.

Figure 10 shows the improved agreement after the peak, which is obtained by the inclusion of a long delay time. The best fit is provided by n equal to 1.5. In Fig. 11, the compensated reactivity obtained from the zero time-delay model is plotted on the ordinate relative units and the time in periods measured from the peak of the burst is given on the abscissa. The theoretical curves, shown in solid lines, are for different values of n. The experimental values are the individual points. The experimental reactivity compensation continues to rise steeply even after the peak of the burst, an effect which is not predicted by the zero-delay model. As shown in Fig. 12, when a long time delay is included in the model the calculated compensated reactivity curves are in accord with the experimental data well past the peak of the burst. The best fit is obtained with n about 1.5.

The solid line in Fig. 13 shows the observed power burst for a transient with an initial period of 7.4 milliseconds. The power is shown on the ordinate in relative units and the time in milliseconds is given on the abscissa. The calculated values for n equal to two are shown by the points. The agreement is satisfactory over almost the entire burst.

Figure 14 displays the results of ramp rate studies with the B-12/64 core. In these experiments reactivity was added at a fixed rate throughout the test. The peak power is shown in megawatts on the ordinate and the initial power is shown on the abscissa. The ramp rates were 0.01% Δk/sec for the bottom line, 0.1% Δk/sec for the middle line and 0.27% Δk/sec for the top line. Figure 15 shows, for the same experiments, the maximum reciprocal period, α, in reciprocal seconds on the ordinate and initial power in watts on

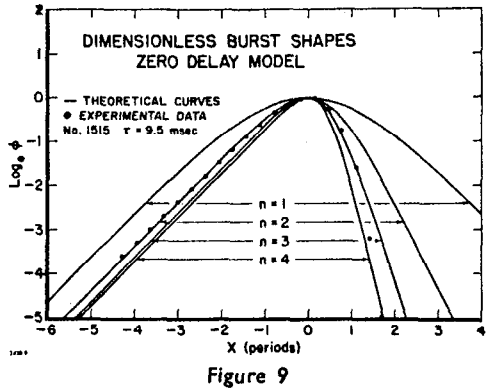

Figure 9

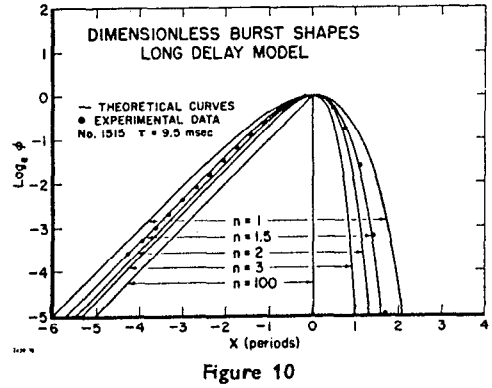

Figure 10

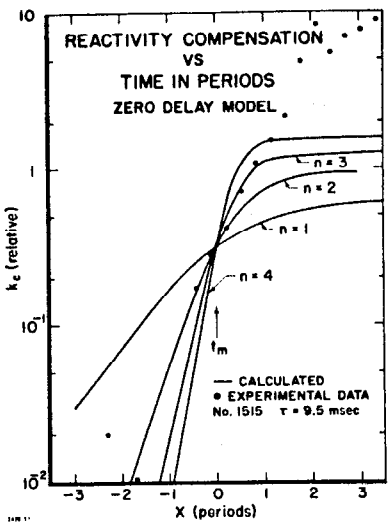

Figure 11

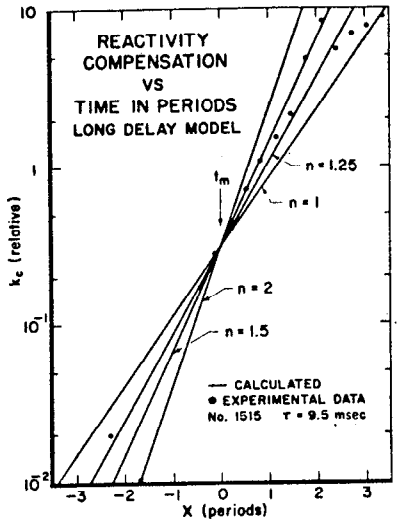

Figure 12

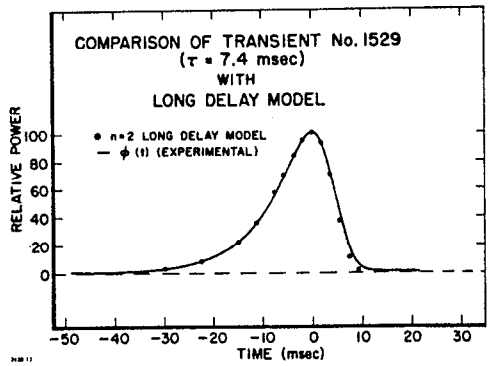

Figure 13

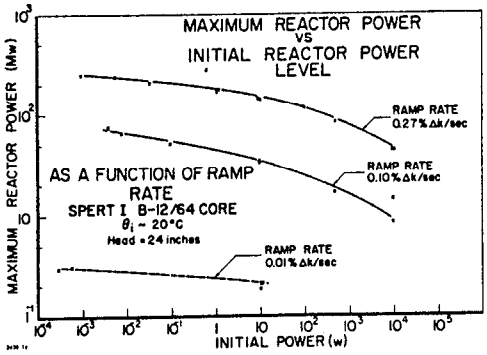

Figure 14

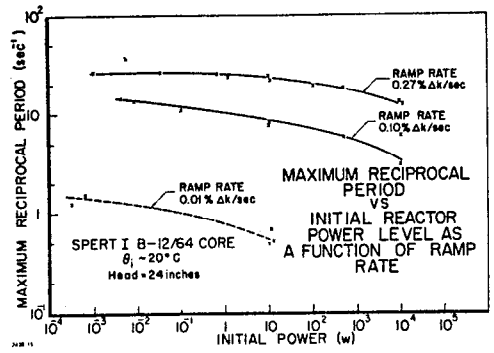

Figure 15

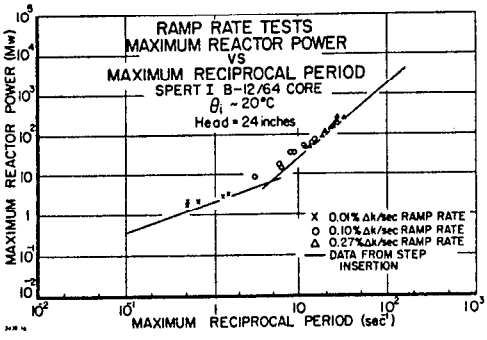

Figure 16

the abscissa. The three lines, from bottom to top, are for ramp rates of 0.01% Δk/sec, 0.1% Δk/sec and 0.27% Δk/sec, respectively.

In Fig. 16, the maximum power in megawatts is plotted on the ordinate against maximum reciprocal period in reciprocal seconds on the abscissa. The crosses, circles and triangles represent ramp-rates of 0.01% Δk/sec, 0.10% Δk/sec and 0.27% Δk/sec, respectively. Also shown as a solid line are the data from step insertions of reactivity. With reasonable accuracy the primary burst of a ramp test with a maximum reciprocal period α_m is equivalent to a step burst with an initial reciprocal period α equal to α_m.

The simple theory implies that, for ramp-induced burst, the power at which the maximum value of the reciprocal period occurs is proportional to the ratio of the ramp rate to the reactivity coefficient. The experimentally observed behavior, however, is more consistent with a weaker dependence on the reactivity coefficient. The assumption required for the step tests, that the reactivity loss is proportional to the nth power of the energy release, also produces agreement for the ramp tests. That is, the simple model used to describe the prompt neutron burst yields results which agree well with the experimental data for both ramp-rate and step reactivity tests.

The theory can be used to predict certain characteristics of power behavior as a function of time. For example, the model for ramp tests with n equal to one indicates that in order for a power maximum to occur during the reactivity insertion, the injection rate must be greater than the product of the reactivity coefficient and the initial power. This condition applies even when delayed neutrons are taken into consideration. The observed reactivity coefficient for the SPERT I core is about -4.0×10^{-2} % Δk/Mw sec. Hence for initial powers above a megawatt, the rate of reactivity injection must be greater than 4.0×10^{-2} % Δk/sec in order to produce a burst. For an initial power of 100 megawatts the required rate would be the rather high rate of 4% per second. It is also possible to estimate the conditions required to produce a burst having any given value of maximum α. For example, for a maximum α of 10 reciprocal seconds, the required ramp rate is about 1% per second at one megawatt, and about 9% per second at 100 megawatts.

In summary, the observed behavior of all the SPERT I cores is predicted for both step and ramp transients by relatively simple theoretical considerations. The theory treats the reactor as a lumped parameter system without specifically including the details of the shutdown process and therefore should be applicable to other reactors of the same general type.